

## ENERGY SPECTRA IN THE NAC PROTON THERAPY BEAM

F D BROOKS<sup>1</sup>, D T L JONES<sup>2</sup>, C C BOWLEY<sup>1</sup>, J E SYMONS<sup>2</sup>, A BUFFLER<sup>1</sup>, and M S ALLIE<sup>1</sup>

<sup>1</sup> Department of Physics, University of Cape Town, Rondebosch, 7700 South Africa

<sup>2</sup> Division of Medical Radiation, National Accelerator Centre, P O Box 72, Faure, 7131 South Africa

In order to tailor a proton beam for radiation therapy several beam modification devices are used which affect both the dose distribution and the energy spectrum of the beam. Knowledge of the proton spectra is required for optimizing the beam delivery system and for comparison with theoretical calculations. Proton elastic scattering has been used to measure spectra in the NAC 200 MeV clinical beam. A polyethylene scatterer is located at the treatment isocentre. Two scintillator detector  $\Delta E/E$  telescopes are placed symmetrically about the beam axis such that the energy of both the scattered and recoil protons is half the incident beam energy. Multiparameter data acquisition and analysis is used to determine the coincident summed spectra under various irradiation conditions.

### 1. Introduction

In order to tailor a proton beam from an accelerator for use in radiotherapy several beam modification devices have to be introduced between the accelerator and the patient. These devices affect both the dose distribution and the energy spectrum of the beam. Monte Carlo and analytic calculations<sup>1</sup> can be undertaken to predict the effect of these devices and thus to ensure beam characteristics optimized for specific therapy requirements. The reliability of these calculations needs to be checked, however, and this can only be done, ultimately, by experimental measurement. Spectral information can also be used in treatment planning programmes and for explaining differences in clinical, radiobiological and dosimetric data obtained at various centres. No energy spectra measurements appear to have been reported for any of the high-energy proton therapy facilities now in operation. At the National Accelerator Centre (NAC) a project is now under way to develop and test a system for measuring spectra in the NAC's 200 MeV proton therapy beam<sup>2,3</sup>. A description of this system is presented here and some preliminary measurements which have been made are discussed.

The beam line has previously been described in detail<sup>2,3,4</sup>. Briefly, a passive double-scatterer and occluding ring system<sup>5,6</sup> is used to spread and flatten the beam. The beam is collimated at several points along the beam line, including a final collimator, situated 31 cm upstream of the treatment isocentre, which is generally shaped specifically for each field to match the tumour shape. In addition there are multi-wire and quadrant (Lawrence Berkeley National Laboratory) ionisation chambers, with feedback systems to steering magnets in order to ensure accurate beam alignment and symmetry, and a pair of parallel plate ionisation chambers for dose monitoring. The reference beam for absolute dose calibrations<sup>7,8</sup> has a 5 cm diameter final collimator and a range (measured to the distal 50% of the Bragg peak) in water of  $24.00 \pm 0.03$  cm, corresponding to an energy of 191 MeV<sup>8,9</sup>. To ensure reproducibility of this range proton beams with slightly higher energies than

required are delivered, and the range is then trimmed by the insertion of  $0.06 \text{ g.cm}^{-2}$  thick plastic plates.

In addition to the above devices, which are always in the beam, acrylic attenuators can be manually inserted in the beam path to adjust the range of the beam to the planned treatment depth. Range modulating acrylic propellers<sup>10</sup> are used to provide spread-out Bragg peaks (SOBP). In the present series of measurements the effects on the spectra of the devices which are patient-specific (final collimators, attenuators and modulators) were investigated.

### 2. Experimental method

A thin polyethylene radiator (30 mm diameter  $\times$  3 mm thick) was mounted at the treatment isocentre. A pair of  $\Delta E$ -E detector telescopes, each consisting of a  $\Delta E$ -detector (25 mm  $\times$  25 mm  $\times$  5 mm thick NE102 plastic scintillator) backed by a full-energy NaI(Tl) E-detector (50 mm diameter  $\times$  125 mm thick), was used to detect the elastically scattered and recoil protons. A diagram of the experimental arrangement is given in Fig. 1. The NaI(Tl) crystals were fitted with thin entrance windows (7  $\mu\text{m}$  Havar) and enclosed in annular lead shields 20 mm thick. Additional shadow-shielding for both telescopes was also provided. The beam and telescope axes were all horizontal and intersected at the treatment isocentre. The telescope axes made equal angles of  $\theta = 44^\circ$  with the beam axis. The distance between the radiator and the entrance window of the NaI(Tl) crystals was 42 cm. Relativistic kinematics gives  $\theta = 43.6^\circ$  as the angle of maximum efficiency for detecting the scattered and recoil protons for 200 MeV incident protons, but the finite angular resolution of the detectors ( $3^\circ$  full width at half maximum (FWHM)) allowed coincidences to be registered for the full range of energies of interest ( $0 < E < 205$  MeV) with  $\theta = 44^\circ$ .

The energy-dependent efficiency factor  $\phi(E)$  due to the relativistic effects mentioned above was determined

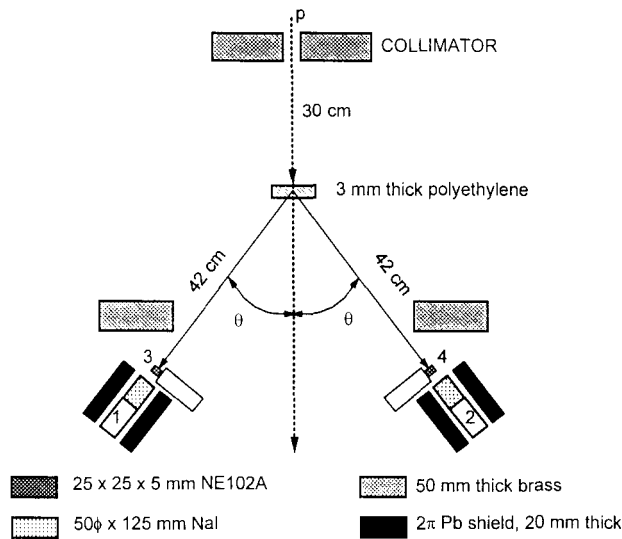


Fig. 1. Diagram of the experimental arrangement.

by calculation.  $\phi(E)$  was found to be a maximum for 84 MeV incident protons, declining to about 80% and 60% of maximum for 20 MeV and for 200 MeV incident protons respectively. The variation in  $\phi(E)$  with  $\theta$  for 200 MeV incident protons was measured to check the validity of the method used in the calculations.

A fourfold coincidence between the scintillators of the two telescopes was required to define an event. An abridged block diagram of the data acquisition system is given in Fig. 2. The four detector pulse heights ( $L_1, L_2, L_3$  and  $L_4$ ) as well as the coincidence time delay ( $T$ ), between the two plastic scintillators, were digitised and written to an event file using the NAC data acquisition system. The electronics also incorporated a LED pulser system to monitor the gain stability of the NaI(Tl) scintillators.

### 3. Data reduction

The data analysis, which was carried out off-line, consisted of applying appropriate windows on the L (Figs. 3,4 and 5) and T parameters in order to select true p-p coincidence events (events for which a scattered proton detected in one telescope is in coincidence with the associated recoil proton detected in the other telescope) and to exclude a large fraction of the "reaction tail" events which occur in the scintillators. For these events the summed pulse heights of the four scintillators, all calibrated to equal gain, then gave the incident proton energy  $E(=E_1+E_2+E_3+E_4)$ . The spectra thus obtained were then corrected for the energy dependence of the detection efficiency of the system. This efficiency,  $\epsilon(E)$ , was assumed to be proportional to the factor  $\phi(E)$  referred to above and to the Rutherford cross section for p-p elastic scattering, which varies as  $E^{-2}$  in the laboratory frame. Thus

$$\epsilon(E) = k \cdot \phi(E) \cdot E^{-2}$$

was assumed, and the constant  $k$  was adjusted so as to normalize the peak intensity of each spectrum to the arbitrary value of 1000 counts per energy bin.

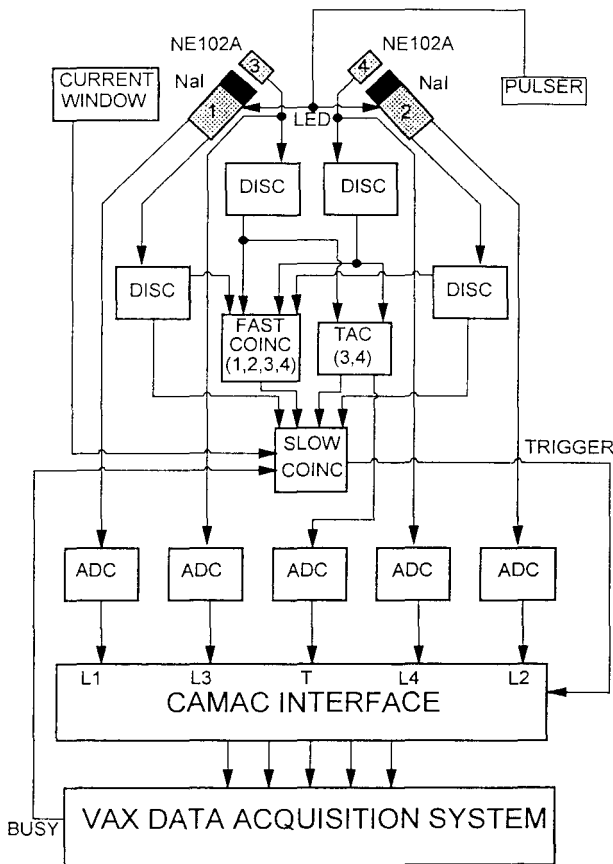


Fig. 2. Abridged block diagram of the data acquisition system.

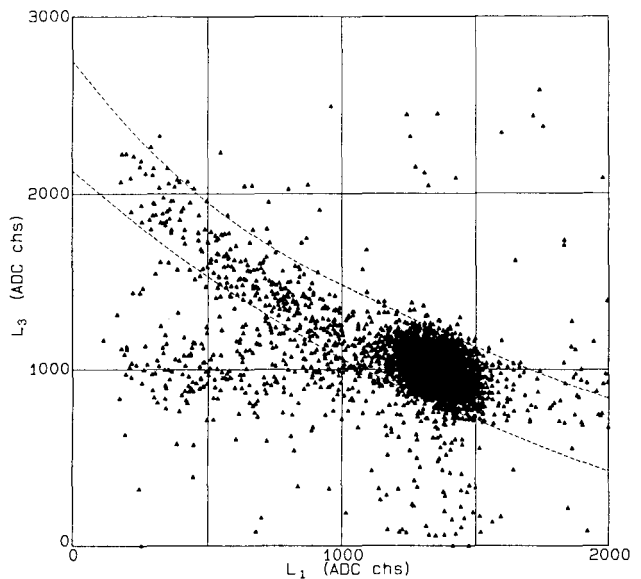


Fig. 3. Scatter plot of coincident events versus pulse heights  $L_1$  and  $L_3$  (from telescope 1-3). The dashed lines show the window used to select proton events and reject reaction tail events.

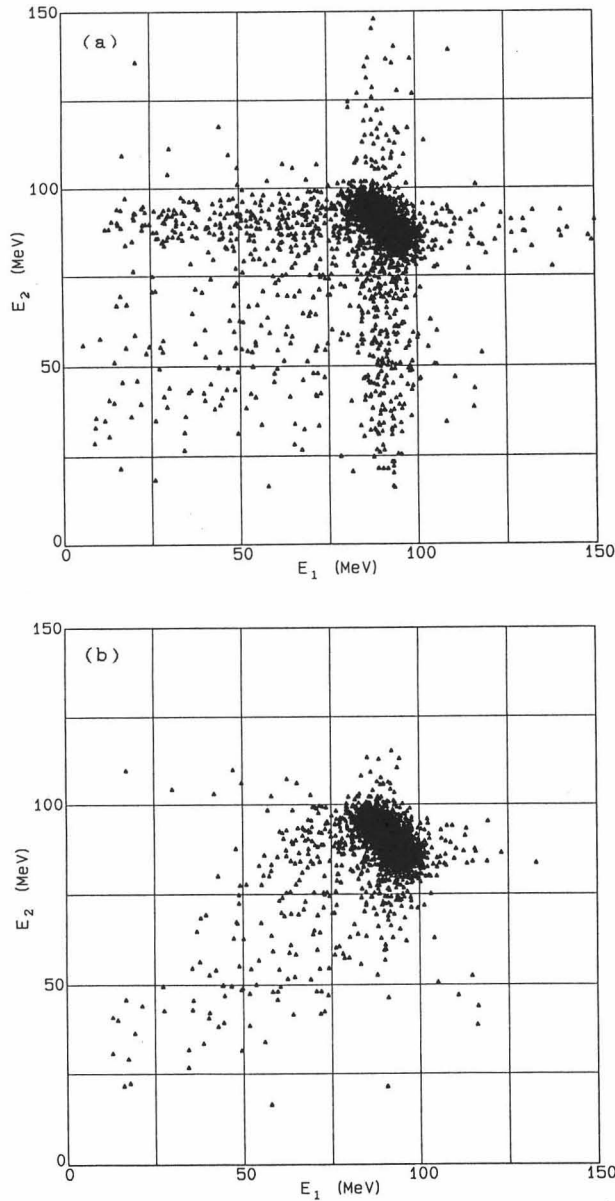


Fig.4. Scatter plots of coincident events versus energies  $E_1$  and  $E_2$ , obtained (a) without imposing; and (b) imposing, proton windows in the two telescopes. The data were taken using a final collimator of diameter  $d=10$  mm, with no other beam modification elements in position.

#### 4. Proton spectra

Unless otherwise stated all data presented here were obtained with the double scatterer beam spreading system in the beam. A summary of the measurements is given in Table 1. The attenuators have the expected effect on the energy spectrum (spectra 2, 3, 4, and 8; with 0, 31, 93, and 119 mm of acrylic in the beam respectively) in that the peak energy decreases and the FWHM increases with increasing thickness (Fig. 6).

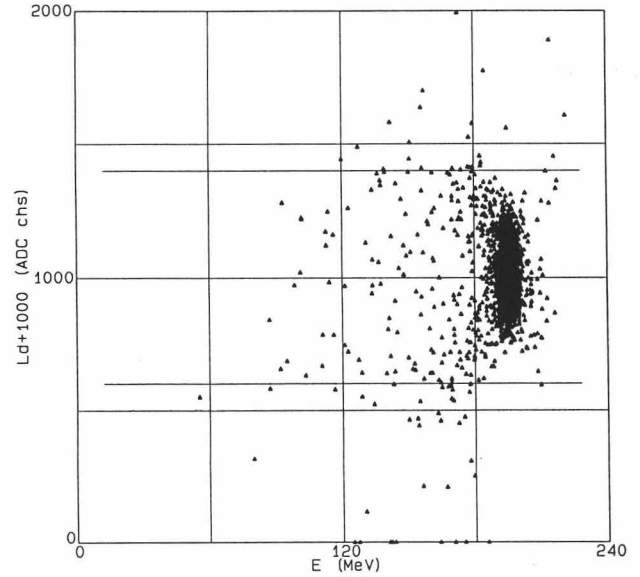


Fig.5. Scatter plot showing the same events as in Fig. 4 (b) ( $d=10$  mm) replotted versus total energy  $E$  and the pulse height difference  $L_d=L_1-L_2+1000$ . The lines at  $L_d=\pm 400$  show the window imposed to select coincidences satisfying the condition  $E_1 \approx E_2$ .

TABLE 1: EXPERIMENTAL MEASUREMENTS.

Spectrum number	Distance from isocentre (mm)	Collimator diameter (mm)	Attenuator thickness (mm acrylic)	SOBP (mm water)	Peak Energy (MeV)	FWHM (MeV)
1	0	10	0	0	190.8	7.8
2	0	50	0	0	190.8	6.6
3	0	50	31	0	174.1	6.7
4	0	50	93	0	134.6	8.5
5	0	50	93	50	134.6	12.3
6	0	50	93	110	134.6	12.3
7	0	50	0	110	190.8	11.0
8	0	50	119	0	91.1	11.5
9	0	100	0	0	190.8	6.6
10	-270	100	0	0	190.8	6.9

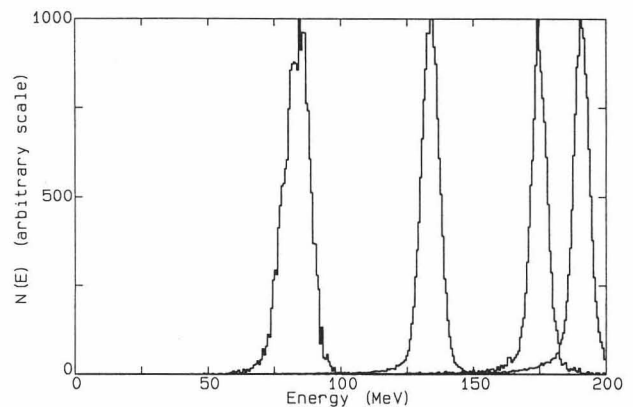


Fig.6. Proton energy spectra measured using the  $d=50$  mm collimator and with 0, 31, 93 and 119 mm thick acrylic degraders in the beam.

Considering the effect of the collimator diameter  $d$  (spectra 1, 2, and 9; with  $d = 10, 50,$  and  $100$  mm respectively) there is a decrease in the FWHM between the 10 mm and 50 mm collimators, but no difference between the 50 mm and 100 mm collimators. This is probably due to the protons which have been scattered off the collimator striking the radiator (diameter of 30 mm) in the case of the 10 mm collimator, but not in the 50 mm and 100 mm cases (Fig. 7).

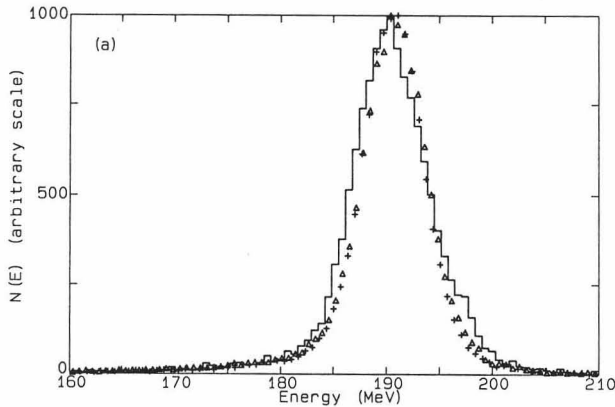


Fig.7. Proton energy spectra measured using collimator diameters  $d=10$  mm (histogram), 50 mm (triangles) and 100 mm (crosses).

The comparison of different modulator wheels (spectra 4, 5, and 6; with 0, 50, and 110 mm SOBPs respectively) shows clearly that the modulator propeller spreads the high energy component of the spectrum, as desired, without introducing any significant additional low energy component. The FWHM with the modulators in the beam (spectra 5 and 6) are the same because the open and thinner sections of the modulator propeller are the same for both cases (Fig. 8).

Moving the scatterer upstream from the isocentre (spectra 9 and 10; 0 and 270 mm upstream respectively) results in an insignificant increase in the FWHM.

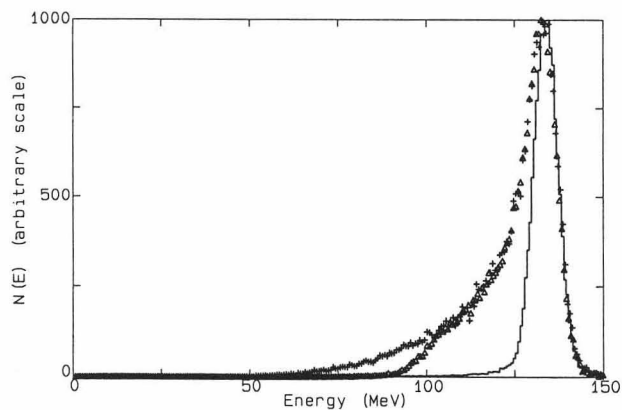


Fig.8. Proton energy spectra measured with the  $d = 50$  mm collimator and with modulator propellers providing 0 mm (histogram), 50 mm (triangles) and 110 mm (crosses) SOBPs.

## 5. Discussion

This system had several advantages: firstly, it enabled measurements to be done in situ in the normal therapy beam at the usual beam currents used for therapy (20 - 80 nA) without pulse pileup problems; secondly, it minimised the "reaction tail" effect caused by protons undergoing nuclear reactions in the scintillators.

A feature of the data is the negligible number of low-energy protons in the spectra. The preliminary measurements have also revealed limitations in the technique, some of which could be reduced or eliminated in future work. The energy thresholds of the NaI(Tl) detectors, for example, could be lower than the values of about 22 MeV used here if the ambient background (mainly from gammas and neutrons) in the experimental area could be reduced significantly. This would make it possible to extend studies of the low-energy component to incident energies below about 60 MeV, the limit imposed by the present thresholds. In order to make measurements at incident proton energies less than 30 MeV (15 MeV in each telescope), it will also be necessary to improve the performance of the  $\Delta E$  detectors.

It has been demonstrated that the method described here is suitable for assessing spectral characteristics of a high-energy proton therapy beam. It should prove useful in providing experimental data to check theoretical calculations on which treatment planning is based.

## References

1. B. Gottschalk, A. M. Koehler, R. J. Schneider, J. M. Sisterson and M.S. Wagner, *HCL Report 11/19/90* (Harvard Cyclotron Laboratory, Cambridge, MA, 1990)
2. D.T.L. Jones, A. N. Schreuder, J.E. Symons and M Yudelev, in: *Hadrontherapy in Oncology*, (Eds. U. Amaldi and B. Larsson, Elsevier Science B.V., 1994) p307
3. D.T.L. Jones, in: *Ion Beams in Tumor Therapy*, (Ed. U Linz, Chapman and Hall, 1995) p350
4. A.N. Schreuder, D.T.L. Jones, J.E. Symons, T. Fulcher, and A. Kiefer, *Proc. 14th Int. Conf. on Cyclotrons and their Applications*, Cape Town, October 1995 (World Scientific, in press).
5. A.M. Koehler, R. J. Schneider and J.M. Sisterson, *Med. Phys.* **4** (1977) 297
6. B. Gottschalk, *Private communication* (1991)
7. S. Vynckier, D.E. Bonnett and D.T.L. Jones, *Radioth. Oncol.* **20** (1991) 53
8. S. Vynckier, D.E. Bonnett and D.T.L. Jones, *Radioth. Oncol.* **32** (1994) 174
9. ICRU Report 49, *Stopping Powers and Ranges for Protons and Alpha Particles*. (International Commission On Radiation Units and Measurements, Bethesda, MD, 1993)
10. A.M. Koehler, R.J. Schneider and J.M. Sisterson, *Nucl. Instr. Meth.* **131** (1975) 437